

Anomalous energy dissipation of electron current pulses propagating through an inhomogeneous collisionless plasma medium

Sharad Kumar Yadav,^{a)} Amita Das,^{b)} Predhiman Kaw, and Sudip Sengupta
Institute for Plasma Research, Bhat, Gandhinagar 382428, India

(Received 28 December 2008; accepted 1 April 2009; published online 20 April 2009)

The evolution of fast rising electron current pulses propagating through an inhomogeneous plasma has been studied through electron magnetohydrodynamic fluid simulations. A novel process of anomalous energy dissipation and stopping of the electron pulse in the presence of plasma density inhomogeneity is demonstrated. The electron current essentially dissipates its energy through the process of electromagnetic shock formation in the presence of density inhomogeneity. A direct relevance of this rapid energy dissipation process to the fast ignition concept of laser fusion is shown. © 2009 American Institute of Physics. [DOI: 10.1063/1.3122939]

The interaction of fast rising electron current pulses with a fully ionized plasma is an important area of research activity. It has applications in areas as diverse as fast ignition (FI) concept of laser fusion, the dynamics of plasma opening switches, the physics of nondiffusive penetration of magnetic fields in astrophysical plasmas, the kinetics of electron layer in collisionless magnetic reconnection phenomena, etc.^{1–6} An issue that is of frontline interest in these contexts is the rate at which the energy associated with the current pulse dissipates in the plasma. For a weakly collisional or collisionless plasma the energy dissipation can occur only through some anomalous process. In this work a novel anomalous energy dissipation is demonstrated for the first time by numerically simulating the two-dimensional (2D) electron magnetohydrodynamic (EMHD) equations describing the propagation of fast rising electron pulse structures through an inhomogeneous plasma.⁷ The mechanism relies on energy dissipation in electromagnetic shock structures which form because of EMHD propagation effects in the presence of plasma density inhomogeneity. A direct relevance of such a process to FI concept of laser fusion is also outlined.

The propagation of a short duration electron current pulse is perceived by the plasma as a propagating low frequency electromagnetic disturbance. The plasma tries to shield itself from this disturbance by inducing return currents. The combination of forward current (due to incoming current pulse) and return shielding currents of the plasma is unstable to fast electromagnetic instabilities known as Weibel instabilities. This instability separates the forward and return currents spatially. This leads to the formation of cylindrical current channels. The center of the cylindrical channel carries the forward current which is surrounded by a cylindrical shell of return plasma current. The flow configuration, thus varies along z and the radial direction, and is independent of θ . This current configuration produces poloidal $\hat{\theta}$ magnetic fields. For convenience a transverse slice of the cylinder is represented by the slab x - z coordinate system. This is strictly valid in the limit when the radius of curvature

of the cylinder is large compared to the typical gradient scales. In this representation the magnetic field associated with the combination of forward and return currents forms two lobes (a dipolar structure) with positive and negative magnetic field directed along y .⁷ Since the dynamical time scale of the phenomena is associated with fast plasma response at electron time scales, this magnetic field configuration can be identified with the axially translating dipole solution of the EMHD equations.^{8,9} We have numerically simulated the propagation of such dipolar configurations in a plasma with strong plasma density gradients.

The density inhomogeneity is incorporated in the EMHD formalism through a recently proposed generalized electron magnetohydrodynamic (G-EMHD) model in 2D x - z plane.⁷ The G-EMHD model in 2D with magnetic field component only along the symmetry direction \hat{y} and inhomogeneity along z , the propagation direction of dipole, can be written as

$$\frac{\partial G}{\partial t} + \frac{1}{n_0} \hat{y} \times \nabla b \cdot \nabla G = G \frac{\partial b}{\partial x} \frac{\partial}{\partial z} \left(\frac{1}{n_0} \right) - \eta \nabla^2 b + \mu \nabla^2 \nabla^2 b, \quad (1)$$

$$G = \frac{1}{n_0} \nabla^2 b - b - \frac{1}{n_0^2} \frac{\partial n_0}{\partial z} \frac{\partial b}{\partial z}.$$

For Eq. (1) we have chosen to normalize the magnetic field and electron density by their typical values B_{00} and n_{00} , respectively. Time is normalized by the electron gyroperiod corresponding to B_{00} , $\omega_{ce0}^{-1} = 1/(eB_{00}/mc)$, length by the electron skin depth $d_{e0} = c/\omega_{pe0}$ (where $\omega_{pe0}^2 = 4\pi n_{00}e^2/m$), and η is the normalized classical resistivity parameter. We have numerically simulated Eq. (1) for a variety of initial configurations and distinct density inhomogeneities. Here we present results for the evolution of an initial configuration of a 2D dipolar structure shown in Fig. 1. The plasma density inhomogeneity has been chosen to have a tangent hyperbolic density profile along z , as shown in the subplots [(g) and (h)] of Fig. 1. The profile thus has homogeneous regions of both low and high densities in the simulation domain separated by a spatial region in which the density varies sharply. The dipole axis is placed parallel to the z direction and it moves toward

^{a)}Electronic mail: sharad@ipr.res.in.

^{b)}Electronic mail: amita@ipr.res.in.

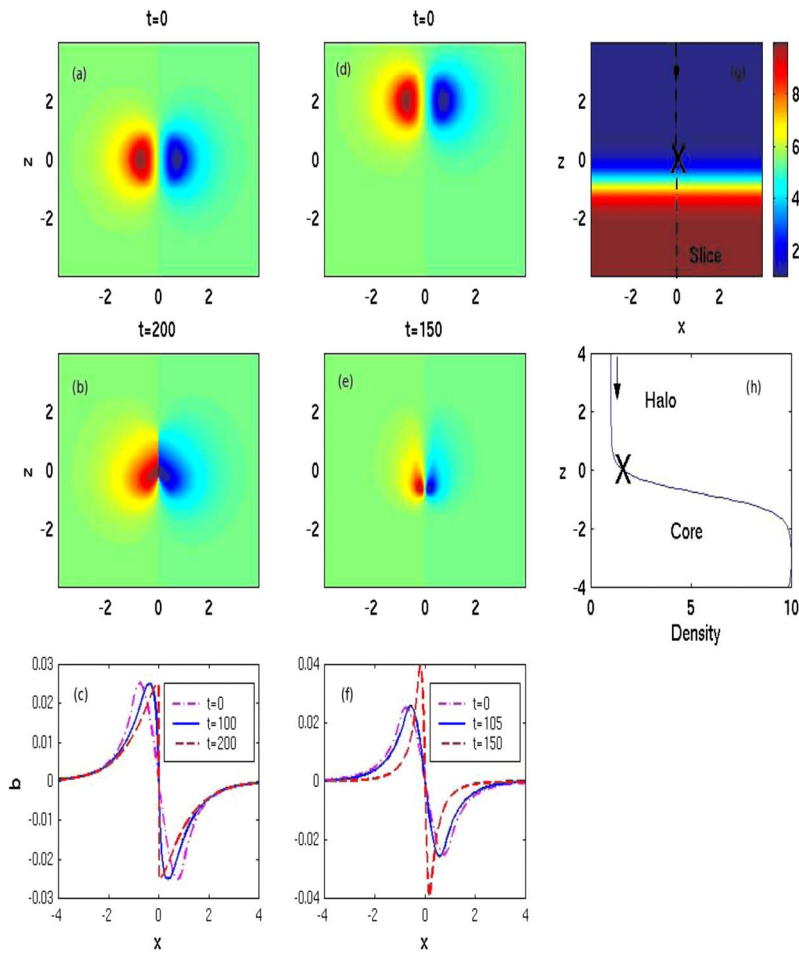


FIG. 1. (Color online) The contour plots of the magnetic field b in the x - z plane is shown in subplots (a) and (b) (inertialess case) (d) and (e) (full G-EMHD) at two different times. The numbers $(-2,0,2)$ on the axis of these plots show length in units of electron skin depth (corresponding to the low density plasma). The magnetic field b profile in x at the midplane of the structure in z has been depicted at various times in subplots (c) and (f) for inertialess and the full G-EMHD simulations respectively. Subplots (g) and (h) show the inhomogeneous plasma density profile through which the dipolar structure evolves. The cross \times and the arrow \rightarrow marks on these subplots show the initial location of the dipole for inertialess (dipole has no axial velocity in this case) and full G-EMHD simulations.

increasing plasma density. The simulations show that as the dipole encounters an increasing plasma density, a transverse drift velocity proportional to the magnetic field at a given location, viz., $\vec{v}_d = -b \partial(1/n_0)/\partial z$ is induced. The sign of magnetic field b being opposite in the two lobes, the lobes drift in opposite direction. While translating toward increasing plasma density they approach each other forming an electromagnetic shock structure. The shock formation can be clearly seen from the constant contour plots of b shown for simulations for the inertialess case as well as that for full G-EMHD equations in Fig. 1. In the inertialess case the shock structure is more prominent. The dipole has no axial velocity for the inertialess case. Thus for this case the structure is kept initially itself at a location where the plasma density gradient exists (the location is shown by the \times symbol in the density profile shown in subplots [(g) and (h)] of Fig. 1). For the simulations with the full G-EMHD equations including inertia terms the dipole has an axial translational speed. In this case as the lobes of the dipoles are pushed closer to each other and their size diminishes, the associated maximum magnetic field increases, as a result of which the dipole translates faster through the inhomogeneous region. The structure, therefore, keeps penetrating toward the higher density region and it also keeps getting sharper. However, once it reaches the plateau of the high density side it again readjusts its shape to a dipolar form corresponding to the local skin depth.

We now evaluate the energy dissipation that occurs as a result of the formation of sharp structure transverse to the plasma density gradient. The energy associated with the dipole structure is the sum of magnetic and electron kinetic energies and is given by the expression $E = \iint (b^2 + (\nabla b)^2/n) dx dz$, which is conserved in the absence of any dissipation. The choice of $\eta = \mu = 0$ ensures that there is no energy dissipation while the structure (resolved well by the spatial grid) moves through the homogeneous region. We observe that as the dipolar magnetic structures translate through the inhomogeneous profile region, the energy E exhibits a sharp fall as shown in subplot (a) of Fig. 2. The timing of this drop in energy content of the dipole is observed to coincide with the interval when the dipolar structure translates past the inhomogeneous plasma density region. This sharp fall in energy is due to the shock formation, which cannot be resolved adequately no matter how fine the resolution is. The value of ΔE is typically the same for different values of the grid resolution Δx . The shock width essentially adjusts itself according to the grid resolution. The total energy dissipation is found to be independent of the value of the grid dissipation. We have also carried out simulations with finite and various values of η and μ . The energy dissipation for these cases has been shown in subplots (b) and (c). It can be seen that in these cases the energy also dissipates while the structure passes through the homogeneous density region of the plasma. However, the drop in

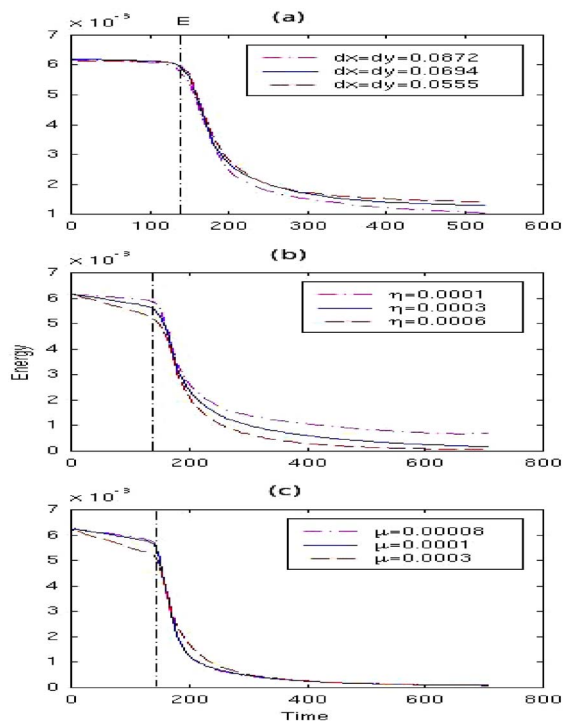


FIG. 2. (Color online) Evolution of the total energy of the structure for full G-EMHD simulations, as it propagates through the inhomogeneous plasma density (a) for various grid resolutions (b) for simulations with finite resistivity parameter η and (c) with finite viscosity parameter μ in G-EMHD equations. A thick dashed vertical line shows the time when the dipole enters the inhomogeneous plasma density region.

energy while the structure moves through the inhomogeneous density region remains approximately the same for different values of η and μ . Also this ΔE compares well with the case of $\eta = \mu = 0$ of subplot (a) of the same figure, where only grid dissipation was operative. We thus find that the energy dissipation is independent of the value as well as the form of dissipation. This, as argued below is due to a suitable adjustment of shock width l_x with the dissipation coefficient. So, even when the dissipation tends toward zero (is negligible) the total energy dissipation remains unaffected.

We now provide a physical understanding of the process of shock formation and also show how the magnitude of energy dissipation would be insensitive to the value of dissipation coefficient. As the two lobes of the dipole approach each other it leads to the steepening of the electron current gradients. The steepening has its origin in the influence of plasma inhomogeneity on the EMHD equations. In the inertialess limit $G = -b$ and Eq. (1) gets simplified to $\partial b / \partial t - b(\partial b / \partial x) \partial(1/n_0) / \partial z = \eta \nabla^2 b$. For a simple density variation of the form $\partial / \partial z(1/n_0) = -K$, (here K , the inverse of the normalized density scale length is assumed to be a positive constant, minus sign signifying an increasing plasma density with z) this is Burger's equation. Burger's equation is known to produce shock structures. Since shock is along x , for small η , we have $\eta \nabla^2 b \sim \eta \partial^2 b / \partial x^2$. The analytical form of the shock structure can be obtained by seeking stationarity in a frame moving with a speed u . Thus, upon replacing $\partial / \partial t$ by

$-u \partial / \partial x$ and integrating with respect to x , we get in the inertialess limit

$$b(x) = \frac{u}{K} + \frac{\sqrt{b_0 K - u}}{K} \tanh \left\{ \frac{b_0 K - u}{2} \left(\frac{x}{\eta} + K_2 \right) \right\}. \quad (2)$$

We have used the condition $b = b_0$, and $db/dx = 0$ at the boundaries. The parameter K_2 is the second constant of integration to be determined from the condition $x = -\infty$, $b = b_0$. It is clear from the expression of b that the layer width $l_x = 2\eta / (b_0 K - u)$ scales linearly with η . The rate of heat dissipation in this sharp layer would be given by

$$Q = \int^a \int^L \int^{l_x} \eta \left(\frac{\partial b}{\partial x} \right)^2 dx dz dy. \quad (3)$$

The range of $z = L$ (the shock length) and y (the third dimension) is the system length along this dimension $= a$. The x coordinate, however, has to be integrated over the layer thickness $l_x \sim \eta$. Retaining only $b_0 K$ in comparison to u we obtain the rate of energy dissipation in the shock structure as

$$Q = \eta \frac{b_0^2 a L}{l_x} = \frac{b_0^3 K L a}{2} = \frac{b_0^2 a^2}{2} K L v_e. \quad (4)$$

Here we have replaced one of the b_0 by av_e to obtain the last equality. Here v_e is the incoming electron velocity. The independence of energy dissipation Q from the magnitude of classical resistivity parameter η in the presence of sharp density gradients is known as the EMHD resistance and has been considered in literature earlier.¹ It is interesting next to see what fraction of the incoming energy gets dissipated in the shock structure in this fashion. The incoming rate of energy influx is $E = (b_0^2 / 2) v_e a^2$, provided one assumes that the typical current configuration has identical extent in the two transverse dimensions at a large distance from the density profile region. Here, for the purpose of estimation only magnetic energy has been considered. Typically, for a structure of the size of electron skin depth, both kinetic and magnetic energies are of similar order. This tells us that a fraction (KL) of the incoming energy gets dissipated in the shock structure of length L . Thus if the shock length is of the order of the inhomogeneity scale length K^{-1} then the entire incoming energy would get dissipated.

We next study the influence of electron inertia related terms. As the density gradient induced drift velocity brings the two lobes of the dipoles toward each other, it causes an enhancement of electron velocity shear in the central region. This enhanced velocity shear region is then susceptible to the Kelvin-Helmholtz-like instability^{10,11} in the presence of electron inertia related terms. This instability essentially manifests through electron inertia dependent nonlinearity $\hat{y} \times \nabla b \cdot \nabla \nabla^2 b$ in the evolution Eq. (1) for G . The instability converts the electron flow energy into fine scale vortices. In three-dimensional (3D) the vortex flows cascade the energy toward finer scales and eventually dissipate into heat through electron Landau damping in the direction parallel to the magnetic field. This effect can be modeled by an anomalous electron viscosity coefficient μ_a . In fact in one of our earlier 3D EMHD simulations,¹¹ it has been shown that the nonlinear stage of the velocity shear driven instability exhibits electro-

magnetic turbulence and produces an effective viscosity μ_a . In the collisionless $\eta=0$ case, this anomalous viscosity μ_a , would play a crucial role and define the shock width. Thus mocking up the electron inertia related effects by an effective viscous dissipation $\sim \mu_a \nabla^2 \nabla^2 b$, we can write an approximate equation in the collisionless limit as $\partial b / \partial t + Kb \partial b / \partial x = -\mu_a \partial^4 b / \partial x^4$. The balance between nonlinear and the dissipation term defines the shock width, which scales as $l_x \sim (\mu_a / Kb)^{1/3}$ here. A net energy dissipation rate Q over a length L in this case is $\sim \int [\mu_a (d^2 b / dx^2)^2 dx] 2\pi a L \sim \mu_a 2\pi a K L b^2 / x^3 \sim 2\pi a K L b^3$. Using, Ampere's law we have $b \sim a v_e$, which gives $Q \sim K L b^2 a^2 v_e$. This leads to a similar conclusion as before about the effectiveness of the shock dissipation mechanism and the independence of the energy dissipation in the shock region from the magnitude of the anomalous viscosity coefficient μ_a .

We now apply our observations to the problem of FI.¹² The FI scheme is essentially a variant of the Inertial confinement scheme for which the tasks of target compression and ignition are carried out separately. In this scheme the electron pulse generated at the critical density surface of the precompressed target by the relativistically intense second laser pulse is employed to create a hot spot in the compressed core for ignition. The observation of higher neutron yield in the scaled down experiments shows the success of this concept.¹³ However, there continue to be doubts on whether the scheme would be successful in the context of full scale experiments, where much higher energy electrons (more than 10 MeV) would be required to stop within a length scale of a few microns in a collisionless plasma. In this context the anomalous stopping mechanism presented in this paper could prove extremely important.

Let us now estimate the typical energy of the electrons that can be stopped through this mechanism. The current I in the channel is related to the magnitude of the magnetic field B through Ampere's law as $B=2I/ac$, where a is the dimension of the channel. The rate of energy dissipation Q can then be expressed in dimensional variables as $Q=(B^2/4\pi)\pi a^2 v_e = I^2 v_e / c^2$, v_e being the electron velocity. Since the rate of energy dissipation is essentially the $I^2 R$ (R the resistance) heating of the system, for this case the resistance would be $R=v_e/c^2$ in cgs units. The effective voltage drop can then be estimated from $V=IR$. The typical magnitude of the electron currents in FI experiments is in the range of several hundreds of kiloamperes, and the electrons typically have relativistic energy, their velocity $v_e \sim c$, the speed of light. $R \sim 1/c \sim 30 \Omega$. This helps in estimating the energy of those electrons which can get stopped by this mechanism for a given value of current in the channel. Thus for a 300 kA of current, electrons with energy as high as 10 MeV can be stopped by this process. This estimate is certainly very exciting as it supports the possibility of heating through electron current pulses for ignition.

We would now like to see whether the energy dissipation observed in our simulations provides an estimate of R which is consistent with the derivation above. The current pulse structure propagates with a normalized velocity $v_N=0.01$. From Fig. 2 a time of $\Delta t_N=100$, the total dissipated energy is $\Delta E_N=5 \times 10^{-3}$ from the figure. The suffix N is used to indi-

cate the normalized values here. This provides us with the value of normalized resistivity as $R_N=5 \times 10^{-3}/0.01=0.5$. For the current pulse structures of the typical dimension of electron skin depth a relationship $\omega_c \sim \omega_p v_e / c$ can be obtained between the typical values of the magnetic fields and the electron velocity v_e . The value of R_N provided above then translates to a resistance of $R \sim 0.5 v_e / c^2 \sim \mathcal{O}(v_e / c^2)$. In the case of FI scenario $v_e \sim c$ which implies that $R \sim 0.5/c = 0.5 \times 30 \Omega = 15 \Omega$, which is in close agreement with the analytical estimate made above.

We have presented a new mechanism of rapid energy dissipation through shock formation for a current pulse moving past an inhomogeneous plasma medium. The mechanism was illustrated through G-EMHD fluid simulations and an analytical understanding was also provided. It is interesting to note that our proposed mechanism is consistent with some recent particle-in-cell simulations¹⁴⁻¹⁶ carried out in the context of propagation of energetic electron current toward the dense target core for the FI plasma. These PIC results show a predominance of heating in the region where density gradient is high (the region where the shock structures form). The role of additional effects arising due to dense plasma, uncompensated charge, relativistic electrons for true FI parameters on this particular mechanism need to be studied. Thus, a more detailed investigation of the mechanism operating in the PIC simulations and comparison with G-EMHD fluid simulations here, promises to be quite rewarding.

This work was financially supported by the DAE-BRNS under Sanction No. 2005/21/7-BRNS/2454.

¹A. S. Kingsep, K. V. Chukbar, and V. V. Yankov, in *Reviews of Plasma Physics*, edited by B. B. Kadomtsev (Consultants Bureau, New York, 1990), Vol. 16 (and references therein).

²A. Fruchtman and L. I. Rudakov, *Phys. Rev. Lett.* **69**, 2070 (1992).

³J. Meyer-ter-Vehn, J. Honorubia, M. Geissler, S. Karsch, F. Krausz, G. Tsakiris, and K. Witte, *Plasma Phys. Controlled Fusion* **47**, B807 (2005).

⁴R. L. Stenzel, J. M. Urrutia, and K. D. Strohmaier, *Phys. Rev. Lett.* **101**, 135002 (2008).

⁵H. Shindo, D. Kudo, and S. Fujii, *Jpn. J. Appl. Phys., Part 2* **41**, L956 (2002).

⁶B. N. Rogers, R. E. Denton, J. F. Drake, and M. A. Shay, *Phys. Rev. Lett.* **87**, 195004 (2001).

⁷S. K. Yadav, A. Das, and P. Kaw, *Phys. Plasmas* **15**, 062308 (2008).

⁸M. B. Isichenko and A. M. Marnachev, *Sov. Phys. JETP* **66**, 702 (1987).

⁹A. Das, *Plasma Phys. Controlled Fusion* **41**, A531 (1999).

¹⁰A. Das and P. Kaw, *Phys. Plasmas* **8**, 4518 (2001).

¹¹N. Jain, A. Das, P. Kaw, and S. Sengupta, *Phys. Lett. A* **363**, 125 (2007).

¹²M. Tabak, J. Hammer, M. E. Glinsky, W. L. Kruer, S. C. Wilks, J. Woodworth, E. M. Cambell, and M. E. Perry, *Phys. Plasmas* **1**, 1626 (1994).

¹³M. H. Key, *Nature (London)* **412**, 775 (2001); R. Kodama, P. A. Norreys, K. Mima, A. E. Dangor, R. G. Evans, H. Fujita, Y. Kitagawa, K. Krushelnick, T. Miyakoshi, N. Miyanaga, T. Norimatsu, S. J. Rose, T. Shozaki, K. Shigemori, A. Sunahara, M. Tampono, K. A. Tanaka, Y. Toyama, T. Yamanaka, and M. Zepf, *ibid.* **412**, 798 (2001); R. Kodama, H. Shiraga, K. Shigemori, Y. Toyama, S. Fujioka, H. Azechi, H. Fujita, H. Habarat, T. Hall, Y. Izawa, T. Jitsuno, Y. Kitagawa, K. M. Krushelnick, K. L. Lancaster, K. Mima, K. Nagai, M. Naki, H. Nishimura, T. Norimatsu, P. A. Norreys, S. Sakabe, K. A. Tanaka, A. Youssef, M. Zepf, and T. Yamanka, *ibid.* **418**, 933 (2002).

¹⁴R. B. Campbell, R. Kodama, T. A. Melhorn, K. A. Tanaka, and D. R. Welch, *Phys. Rev. Lett.* **94**, 055001 (2005).

¹⁵J. J. Honorubia and J. Meyer-ter-Vehn, *Nucl. Fusion* **46**, L25 (2006).

¹⁶M. Honda, J. Meyer-ter-Vehn, and A. Pukhov, *Phys. Rev. Lett.* **85**, 2128 (2000); *Phys. Plasmas* **7**, 1302 (2000).